Pion photoproduction and Compton scattering in the cloudy bag model

M. Weyrauch

National Institute for Nuclear Physics and High Energy Physics, Section K (NIKHEF-K), P.O. Box 41882,
NL-1009 DB Amsterdam, The Netherlands
(Received 15 September 1986)

We extend a version of the cloudy bag model, which has successfully been applied previously to describe pion scattering, to also account for pion photoproduction and Compton scattering. Numerical results for the $M_{1+}(T=\frac{3}{2})$ multipole of the photoproduction amplitude and the f_{MM}^{1+} multipole of the photon scattering amplitude are presented and compared to experiments. A comparison is made with other treatments of these processes.

I. INTRODUCTION

For about ten years the cloudy bag model (CBM) has been studied in an attempt to understand the structure of baryons. In this model the three-quark core of the baryon is surrounded by pions coupled in such a way as to restore chiral symmetry, which would otherwise be broken on the bag surface.

One of the first problems studied in the CBM was pion-nucleon scattering,[1] and since then a whole series of investigations on meson-baryon scattering in different versions of the CBM followed.[2-4] Furthermore, there were efforts to understand the electromagnetic properties of the baryons from these models.[5] Photoproduction and Compton scattering off the nucleon are closely related to pion scattering, since both processes involve the full off-shell pion scattering amplitude. Moreover, by unitarity and time-reversal invariance these processes are closely linked to each other. These relations are formulated by Watson's theorem,[6] connecting (π,π) and (γ,π), and by the optical theorem, which links the Compton-scattering amplitude to the total photoabsorption cross section.

These connections make it desirable to describe the three processes simultaneously—a goal which is attempted in this work. While pion photoproduction has already been treated in some versions of the CBM (Refs. 7 and 8), there seems to exist no previous study of photon scattering in this framework. The investigation of Compton scattering together with the other reactions is particularly attractive, since after having fixed the parameters of the model to describe pion scattering and photoproduction the calculation of photon scattering is free of any additional parameters. Fortunately, there are some data available to compare our results with, and there is a good chance that better data will become available as soon as improved photon-beam facilities come into operation.[9]

In this work we do not propose a new version of the CBM, but rather apply one model, which has been successfully used to describe pion scattering, to the $\gamma\pi$ and $\gamma\gamma$ processes. In this model the observed Δ resonance comes about by the Chew-Low process (i.e., rescattering of the pion at the nucleon), the "elementary" Δ excitation (quark spin-isospin flip) and the interference of the two processes. We consider both these elementary processes

also in the case of (γ,π) and in addition study the pion-pole term as predicted by the model. The same dynamics enters the calculation of photon scattering. In this paper we only consider the $M_{1+}(T=\frac{3}{2})$ multipole for (γ,π) and the Compton-scattering f_{MM}^{1+} multipole. A study of other multipoles is under way. Of course, the spin$=\frac{3}{2}$ multipoles have been selected, since they are the most prominent in the Δ-resonance region, on which we concentrate here.

We now would like to briefly comment on the version of the CBM we are dealing with here. The Lagrangian of this model is given—in terms of quark degrees of freedom—explicitly in Ref. 2. From this Lagrangian one then derives the $\pi N, \pi\Delta$ and the $\gamma N, \gamma\Delta$ couplings. If one then eliminates the quark degrees of freedom in favor of effective baryon degrees of freedom, one gets a set of rules for the couplings (including form factors), which are quite similar to those used in phenomenological approaches, which do not introduce quark degrees of freedom at all (e.g., an isobar model supplemented with the Chew-Low process). For convenience and to set some conventions we have reproduced these rules in an appendix. Unfortunately, because an MIT bag is used to model confinement, one is not able to calculate the nucleon, Δ, and πN propagators from the quark model. These are introduced phenomenologically and, in fact, we use a different πN propagator than Ref. 2. Renormalization of the propagators and of the different vertices is treated as in this reference.

The CBM version considered here has been criticized because it does not predict pion s-wave scattering.[3,10] Nevertheless, this model has been quite successful describing pion scattering in the 33 channel, and we do not expect that the model dependence of our results will be strong for the multipoles considered here. But a careful treatment of photoproduction and Compton scattering also in other versions of the CBM will be necessary, especially if one wants to study other partial waves, too.

In Sec. II of this paper we will briefly review the form of the scattering and production amplitudes and the equations they obey, define the πN propagator to be used, and give some useful kinematical relations. The explicit solution of the (γ,π) and (γ,γ) scattering equations will be presented in Sec. III together with a summary of the re-

normalization procedure used. The numerical results are presented and discussed in Sec. IV, followed by a conclusion and a brief outlook.

II. SCATTERING AMPLITUDES

In this section we will set up the basic scattering equations for both pion production and Compton scattering. The important point is, that both processes are closely linked to pion scattering as already alluded to in the Introduction, and we deal here with a description which treats all these processes simultaneously.

A. Basic scattering equations

The scattering equation for the processes under consideration is the (coupled) Lippmann-Schwinger equation

$$T = V + VGT .$$ (1)

The transition matrix T is a 2×2 matrix with the channel transition matrices as entries:

$$T = \begin{bmatrix} t_{\pi\pi} & t_{\pi\gamma} \\ t_{\gamma\pi} & t_{\gamma\gamma} \end{bmatrix} .$$ (2)

The channels are pion scattering $t_{\pi\pi}$, pion photoproduction $t_{\pi\gamma}$, its inverse $t_{\gamma\pi}$, and photon scattering $t_{\gamma\gamma}$. Similarly, the driving potential V is represented by the matrix

$$V = \begin{bmatrix} v_{\pi\pi} & v_{\pi\gamma} \\ v_{\gamma\pi} & v_{\gamma\gamma} \end{bmatrix} .$$ (3)

The propagator G in Eq. (1) will be specified later.

The above coupled equations can be decoupled in terms of the off-shell pion scattering t matrix

$$t_{\pi\pi} = v_{\pi\pi} + v_{\pi\pi} G t_{\pi\pi} ,$$ (4)

if we confine electromagnetic processes to second order in the coupling constant e:

$$t_{\pi\gamma} = v_{\pi\gamma} + t_{\pi\pi} G v_{\pi\gamma} ,$$ (5)

$$t_{\gamma\gamma} = v_{\gamma\gamma} + v_{\gamma\pi} G t_{\pi\gamma}$$

$$= v_{\gamma\gamma} + v_{\gamma\pi} G v_{\pi\gamma} + v_{\gamma\pi} G t_{\pi\pi} G v_{\pi\gamma} .$$ (6)

That means that once we have obtained a solution of Eq. (4), we immediately get solutions for $t_{\pi\gamma}$ and $t_{\gamma\gamma}$, provided we have a model to construct the driving potentials $v_{\pi\gamma}$ and $v_{\gamma\gamma}$. The potentials will be constructed in the cloudy bag model as detailed in the following section. A pictorial representation of Eqs. (5) and (6) is provided by Fig. 1. We will explicitly show later that the formalism used here does indeed automatically satisfy Watson's theorem and the optical theorem. This, of course, is a direct consequence of the fact that the Lippmann-Schwinger equation satisfies two-particle unitarity and that V is constructed to satisfy time-reversal invariance.

B. Partial waves

In practice we project the above equations into partial waves thereby reducing the three-dimensional integral equations into one-dimensional ones. Furthermore we
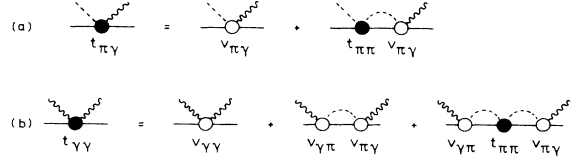

FIG. 1. The photoproduction amplitude Eq. (5) and the Compton-scattering amplitude Eq. (6). The full circles represent amplitudes and the open circles driving potentials. Photons are represented by wiggly lines, pions by dashed lines, nucleons by full lines, and Δ's by open boxes throughout all figures.

concentrate in this paper on the $J = \frac{3}{2}$ partial wave of the πN and γN final states, respectively.

To define our notations and conventions we will collect here explicit formulas for $J = \frac{3}{2}$. For pion scattering we have

$$t_{\pi\pi}^{33}(\mathbf{q}',\mathbf{q}) = 4\pi P_{33}(\hat{\mathbf{q}}',\hat{\mathbf{q}}) t_{\pi\pi}^{33}(q',q)$$ (7)

with $\mathbf{q}$ and $\mathbf{q}'$ the momenta of the incoming and scattered pions, respectively, and P_{33} the projection operator into the $(J = \frac{3}{2}, T = \frac{3}{2})$ partial wave:[11]

$$P_{33}(\hat{\mathbf{q}}',\hat{\mathbf{q}}) = [2\hat{\mathbf{q}}' \cdot \hat{\mathbf{q}} - i\boldsymbol{\sigma} \cdot (\hat{\mathbf{q}}' \times \hat{\mathbf{q}})] T_{\alpha\beta}^3 ,$$ (8)

$$T_{\alpha\beta}^3 = \frac{2}{3}\delta_{\alpha\beta} - \frac{i}{3}\epsilon_{\alpha\beta\gamma}\tau_\gamma .$$ (9)

Analogously one defines, for photoproduction,

$$t_{\pi\gamma}^{33}(\mathbf{q}',\mathbf{k}) = (\hat{\boldsymbol{\epsilon}}_\lambda \times \hat{\mathbf{k}}) \cdot (2\hat{\mathbf{q}}' - i\boldsymbol{\sigma} \times \hat{\mathbf{q}}') T_{\alpha3}^3 t_{\pi\gamma}^{33}(q',k) .$$ (10)

Here $\mathbf{k}$ is the momentum of the incoming real photon and ϵ_λ the polarization vector. Transversality requires $\boldsymbol{\epsilon}_\lambda \cdot \mathbf{k} = 0$. For photon scattering we define the $J = \frac{3}{2}$ partial-wave amplitude by

$$t_{\gamma\gamma}^3(\mathbf{k}',\mathbf{k}) = \{ 2(\hat{\boldsymbol{\epsilon}}_{\lambda'}^{\prime *} \times \hat{\mathbf{k}}') \cdot (\hat{\boldsymbol{\epsilon}}_\lambda \times \hat{\mathbf{k}})$$

$$- i\boldsymbol{\sigma} \cdot [(\hat{\boldsymbol{\epsilon}}_{\lambda'}^{\prime *} \times \hat{\mathbf{k}}') \times (\hat{\boldsymbol{\epsilon}}_\lambda \times \mathbf{k})] \} t_{\gamma\gamma}^3(k',k)$$ (11)

in terms of the momenta and polarizations of the incoming and scattered photons. As is obvious from Eqs. (10) and (11), we are dealing here with a purely magnetic excitation of the system.

We now specify the form of the πN propagator to be used in our calculations. In the c.m. frame Eq. (1) takes the form

$$T(\mathbf{q}',\mathbf{q},E) = V(\mathbf{q}',\mathbf{q},E)$$

$$+ \int \frac{d^3\lambda}{(2\pi)^3} \frac{M}{E_\lambda} \frac{V(\mathbf{q}',\boldsymbol{\lambda},E)T(\boldsymbol{\lambda},\mathbf{q},E)}{E - E_\lambda - \omega_\lambda + i\epsilon}$$ (12)

implicitly defining the propagator G. Here we have introduced the nucleon's mass M, its energy $E_q = \sqrt{M^2 + q^2}$, the pion energy $\omega_q = \sqrt{q^2 + m^2}$, the pion mass m, and the total c.m. energy E.

To relate $t_{\pi\gamma}$ and $t_{\gamma\gamma}$ to more conventional quantities,

we note the following relations, which hold in the c.m. frame:

$$M_{1+}^{3/2} = M_{1+}(T=\tfrac{3}{2}) = \frac{\sqrt{\omega_{q'}k}}{2\pi}\frac{M}{E}t_{\pi\gamma}^{33}(q',k) , \tag{13}$$

$$f_{MM}^{1+} = \frac{k}{2\pi}\frac{M}{E}t_{\gamma\gamma}^{3}(k,k) . \tag{14}$$

The label MM indicates, that excitation as well as deexcitation of the nucleon is magnetic.[12]

Defining the pion-scattering 33 phase shift δ_{33} via

$$t_{\pi\pi}^{33} = |t_{\pi\pi}^{33}|e^{i\delta_{33}} . \tag{15}$$

Watson's theorem states that

$$M_{1+}^{3/2} = |M_{1+}^{3/2}|e^{i\delta_{33}} . \tag{16}$$

Furthermore we have the optical theorem relating f_{MM}^{1+} to M_{1+} by[13]

$$\mathrm{Im}f_{MM}^{1+} = q'\sum_{\alpha}|M_{1+}^{3/2}T_{\alpha3}^{3}+M_{1+}^{1/2}T_{\alpha3}^{1}|^{2} . \tag{17}$$

As can be seen, in the last equation there also enters the $J=\tfrac{3}{2}$, $T=\tfrac{1}{2}$ partial wave, which we will neglect in this paper due to its smallness compared to the $T=\tfrac{3}{2}$ partial wave.

We finally note some useful formulas relating the above-defined amplitudes to observables, if only those partial waves would contribute:

$$\left\langle\frac{d\sigma_{\gamma\gamma}}{d\Omega}\right\rangle = |f_{MM}^{1+}|^{2}\tfrac{1}{2}(7+3\cos^{2}\theta) , \tag{18}$$

$$\sigma_{\gamma}^{\mathrm{abs}} = \frac{8\pi}{k}\mathrm{Im}f_{MM}^{1+}(k,k)$$

$$= 8\pi\frac{q}{k}\sum_{\alpha}|M_{1+}^{3/2}T_{\alpha3}^{3}|^{2} . \tag{19}$$

III. SOLUTION OF THE SCATTERING EQUATIONS

In this section we will derive the driving potentials for the integral equations in the $J=\tfrac{3}{2}$ channel for pion photoproduction and Compton scattering. In terms of these potentials the explicit solutions of the scattering equations will be written down. Furthermore, vertex and mass renormalizations will be briefly discussed. To simplify notation we have dropped the spin and isospin indices in this section, since we are exclusively dealing with the 33 channel here.

A. Driving potentials for the $\pi\pi$, $\gamma\pi$, and $\gamma\gamma$ processes

For convenience and later reference we will briefly recall the driving potentials for pion scattering as first derived by Théberge et al.[2] The $\pi\pi$ process is driven by two potentials corresponding to the Chew-Low process [i.e., the crossed Born term $v_{\mathrm{CL}}^{\pi\pi}$, Fig. 2(a)] and the "elementary" Δ excitation $v_{\Delta}^{\pi\pi}$ [Fig. 2(b)]:
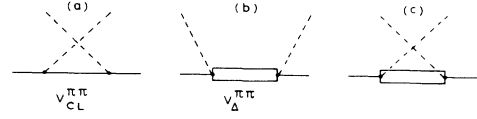

FIG. 2. Driving potentials for pion scattering: (a) crossed Born-term (Chew-Low potential), (b) "bare" Δ, (c) crossed "bare" Δ, which is neglected in this calculation.

$$v_{\pi\pi} = v_{\mathrm{CL}}^{\pi\pi} + v_{\Delta}^{\pi\pi} , \tag{20}$$

$$v_{\mathrm{CL}}^{\pi\pi}(q',q) = \omega g(q')g(q) , \tag{21}$$

$$v_{\Delta}^{\pi\pi}(q',q) = \frac{h(q')h(q)}{E-m_{\Delta}^{(0)}} , \tag{22}$$

with the pion couplings

$$g(q) = i\left[\frac{2}{3}\right]^{1/2}\frac{f_{\pi NN}^{(0)}}{m}\frac{q}{\omega_{q}}\frac{u(q)}{\sqrt{\omega_{q}}} ,$$

$$h(q) = \frac{1}{\sqrt{6}}\frac{f_{\pi N\Delta}^{(0)}}{m}q\frac{u(q)}{\sqrt{\omega_{q}}} . \tag{23}$$

The pion vertices are written in terms of the "bare" πNN and $\pi N\Delta$ coupling constants and the form factor $u(q)$ as defined in the Appendix. The cutoff of this form factor is determined by the bag radius R.

The crossed Δ graph [Fig. 2(c)], which also contributes in the 33 channel, is omitted due to its smallness. As usual we have approximated the nucleon propagator entering (21) by

$$\frac{1}{E-E_{|\mathbf{q}'-\mathbf{q}|}-\omega_{q'}-\omega_{q}} \approx -\frac{\omega}{\omega_{q'}\omega_{q}} \tag{24}$$

defining the on-shell pion energy ω.

In the same version of the CBM we now calculate the driving potentials for the $\gamma\pi$ process $(v_{\pi\gamma})$. Here arises additionally the pion-pole term $(v_{\mathrm{pp}}^{\pi\gamma})$. These potentials are graphically represented in Fig. 3. Using the rules from the Appendix one gets

$$v_{\pi\gamma} = v_{\mathrm{CL}}^{\pi\gamma} + v_{\Delta}^{\pi\gamma} + v_{\mathrm{pp}}^{\pi\gamma} , \tag{25}$$

$$v_{\mathrm{CL}}^{\pi\gamma}(q',k) = \omega g(q')a(k) , \tag{26}$$

$$v_{\Delta}^{\pi\gamma}(q',k) = \frac{h(q')b(k)}{E-m_{\Delta}^{(0)}} . \tag{27}$$
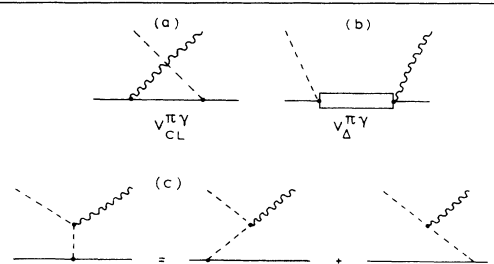

FIG. 3. Driving potentials for pion photoproduction in the 33 channel: (a) crossed Born-term, (b) "bare" Δ, (c) pion-pole term.
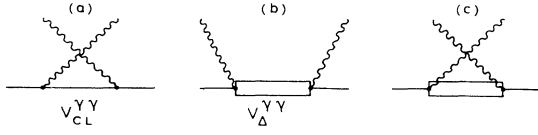
FIG. 4. Driving potentials for Compton scattering: (a) crossed Born-term, (b) "bare" Δ, (c) crossed "bare" Δ, which is neglected in this calculation.

The γNN and $\gamma N\Delta$ vertices are defined by

$$a(k) = i \left[\frac{8\pi}{3k} \right]^{1/2} \frac{e\kappa^{(0)}}{2M} ,$$

$$b(k) = \left[\frac{2\pi k}{3} \right]^{1/2} \frac{f^{(0)}_{\gamma n\Delta}}{m} . \tag{28}$$

The bare couplings $\kappa^{(0)}$ and $f^{(0)}_{\gamma N\Delta}$ can be calculated in the CBM and are given by

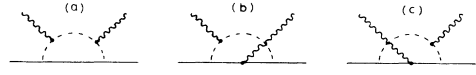$$\kappa^{(0)} = \tfrac{5}{6} \mu_Q 2M \tag{29}$$

FIG. 5. Examples of contributions to Compton scattering, which are automatically generated by iterating the basic photoproduction potentials.

and

$$\frac{f^{(0)}_{\gamma N\Delta}}{m} = e\mu_Q \sqrt{2}, \quad \mu_Q = \frac{R(4\Omega - 3)}{12\Omega(\Omega - 1)}, \quad \frac{e^2}{4\pi} = \frac{1}{137} , \tag{30}$$

$\kappa^{(0)}$ is the "bare" isovector magnetic moment of the nucleon. The magnetic moment of the quark core μ_Q depends on the bag radius R and the frequency of the lowest mode in the MIT bag v ($\Omega = vR = 2.04$). The quark mass is assumed to be zero. Renormalization of $\kappa^{(0)}$ and $f^{(0)}_{\gamma N\Delta}$ will be discussed later. As is obvious from Eqs. (22) and (27) the "bare" Δ has no width, but will acquire its width dynamically.

The pion-pole term [Fig. 3(c)] is in the c.m. frame given by (before projecting out the $J = \tfrac{3}{2}$ partial wave)

$$v^{\pi\gamma}_{pp}(\mathbf{q}',\mathbf{k}) = \hat{\boldsymbol{\epsilon}}_\lambda \cdot \mathbf{q}' \, \boldsymbol{\sigma} \cdot (\mathbf{q}' - \mathbf{k}) \epsilon_{\alpha\beta3} \tau_\beta \left[\sqrt{4\pi} \frac{e f^{(0)}_{\pi NN}}{m} \right] \frac{2}{\sqrt{k\omega_{q'}}} \frac{u(|\mathbf{q}' - \mathbf{k}|)}{\omega^2_{|\mathbf{q}'-\mathbf{k}|}} , \tag{31}$$

and here the projection into the $M^{3/2}_{1+}$ multipole is a bit more involved due to the $\mathbf{q}' - \mathbf{k}$ dependence of this term. After some angular-momentum algebra we find, for the 33 partial wave,

$$v^{\pi\gamma}_{pp}(q',k) = - \left[\sqrt{4\pi} \frac{e f^{(0)}_{\pi NN}}{m} \right] \frac{3}{4} \left[\frac{k}{\omega_{q'}} \right]^{1/2} q' \sum_L b_L(q',k) ,$$

$$b_L(q',k) = (2L+1) \begin{bmatrix} L & 1 & 1 \\ 0 & 0 & 0 \end{bmatrix} \begin{Bmatrix} 1 & 1 & L \\ 1 & 1 & 1 \end{Bmatrix} \int^1_{-1} dx \frac{u(\sqrt{q'^2 + k^2 - 2q'kx})}{q'^2 + k^2 - 2q'kx + m^2} P_L(x) , \tag{32}$$

with $P_L(x)$ the usual Legendre polynomials. To correctly project out the M_{1+} partial wave is important for the numerical results to be obtained. For the $\gamma\gamma$ process in the $J = \tfrac{3}{2}$ channel we consider the two potentials as depicted in Figs. 4(a) and 4(b). We again neglect the crossed Δ graph [Fig. 4(c)] and, of course, neglect direct iteration of the graphs in Fig. 4, since we are only working to order e^2. If we again use the approximation (24) for the nucleon propagator these potentials read

$$v^{\gamma\gamma}_{CL}(q',q) = \frac{\omega}{4\pi} a(q') a(q) , \tag{33}$$

$$v^{\gamma\gamma}_\Delta(q',q) = \frac{1}{4\pi} b(q') b(q) , \tag{34}$$

in terms of the previously defined photon couplings a and b.

Note, that, e.g., graphs as in Fig. 5 need not to be considered as driving potentials, but are automatically generated as iterations of the pion-pole term and interferences of the pion-pole term with v_{CL}. We will further comment on this issue in the next subsection after having established the solution for $t_{\gamma\gamma}$.

B. Solutions for $t_{\pi\gamma}$ and $t_{\gamma\gamma}$

The explicit solution of the pion-scattering equation (4) can be obtained analytically, if all driving potentials are separable as is the case here due to the approximation (24). For convenience and further reference we will here briefly reproduce the result first obtained in Ref. 2:

$$t_{\pi\pi}(q',q,E) = \frac{N(q',q,E)}{D(E)} , \tag{35}$$

$$N(q',q,E) = g(q')g(q)\omega D_2(E) + h(q')h(q)D_1(E)$$

$$+ [g(q')h(q) + h(q')g(q)]\omega D_3(E) , \tag{36}$$

$$D(E) = D_1(E) \cdot D_2(E) - \omega D_3^2(E) . \tag{37}$$

The propagators D_1, D_2, and D_3 are slightly different as compared to Ref. 2, since we are using a different πN propagator. We have listed them in the Appendix. An easy calculation then proves that $\mathrm{Im}N(q',q) = 0$ for the on-shell scattering amplitude. That means that the phase of $t_{\pi\pi}$ is determined by $D(E)$ alone.

Using the result (35) it is lengthy but straightforward to also obtain solutions for $t_{\pi\gamma}$ and $t_{\gamma\gamma}$. In terms of the "bare" γNN and $\gamma N\Delta$ vertices a and b as defined by Eqs. (26) and (27) $t_{\pi\gamma}$ can be written as

$$t_{\pi\gamma}(q',k,E) = \frac{1}{D(E)}\{ [g(q')a(k) + g(q')e(k,E)]\omega D_2(E) + [h(q')b(k) + h(q')f(k,E)]D_1(E)$$

$$+ [g(q')b(k) + h(q')a(k) + g(q')f(k,E) + h(q')e(k,E)]\omega D_3(E) + v_{pp}^{\pi\gamma}D(E)\} \tag{38}$$

with

$$e(k,E) = \frac{2}{\pi} \int d\lambda\, \lambda^2 \frac{M}{E_\lambda} \frac{g(\lambda)v_{pp}^{\pi\gamma}(\lambda,k)}{E - E_\lambda - \omega_\lambda + i\epsilon} , \tag{39}$$

$$f(k,E) = \frac{2}{\pi} \int d\lambda\, \lambda^2 \frac{M}{E_\lambda} \frac{h(\lambda)v_{pp}^{\pi\gamma}(\lambda,k)}{E - E_\lambda - \omega_\lambda + i\epsilon} . \tag{39'}$$

At this stage it is not difficult to prove that Watson's theorem is indeed satisfied by Eq. (38). To this end one first shows that on the mass shell the expression in curly brackets in Eq. (38) has a vanishing imaginary part, so that again the phase is determined by $D(E)$ alone. Therefore $t_{\pi\pi}$ and $t_{\pi\gamma}$ do have the same phase as is required by Watson's theorem.

In a similar fashion we finally obtain the solution for $t_{\gamma\gamma}$:

$$t_{\gamma\gamma}(k',k,E) = \frac{1}{4\pi D(E)}[A(k',k,E)\omega D_2(E) + B(k',k,E)D_1(E) + C(k',k,E)\omega D_3(E) + S(k',k,E)D(E)] \tag{40}$$

with terms corresponding to the Chew-Low process, the elementary Δ excitation, and their interferences with the pion-pole term [Figs. 6(a) and 6(b)]

$$A(k',k,E) = a(k')a(k) + e(k',E)e(k,E) + a(k')e(k,E) + e(k',E)a(k) , \tag{41}$$

$$B(k',k,E) = b(k')b(k) + f(k',E)f(k,E) + b(k')f(k,E) + f(k',E)b(k) , \tag{42}$$

an interference term [Fig. 6(c)]

$$C(k',k,E) = a(k')b(k) + f(k',E)e(k,E) + a(k')e(k,E) + a(k')f(k,E) + b(k')e(k,E) + (k'\leftrightarrow k) , \tag{43}$$
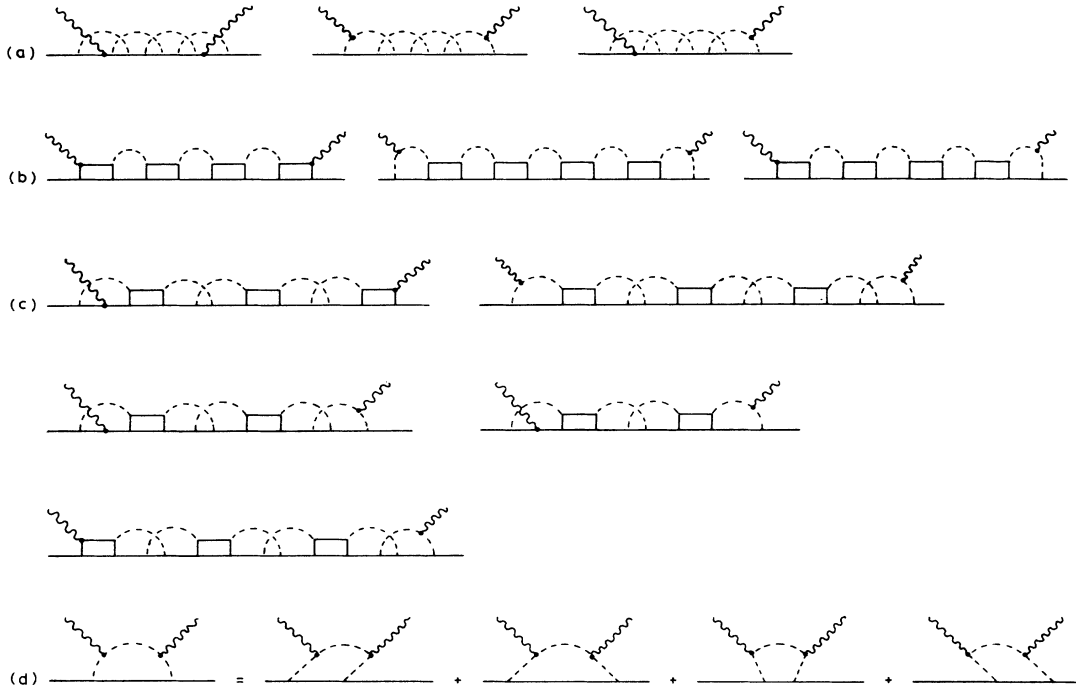

FIG. 6. Graphical representation of the Compton-scattering amplitude Eq. (40): (a) contributions generated by $A(k',k,E)$, (b) contributions generated by $B(k',k,E)$, (c) contributions generated by $C(k',k,E)$, the exchange graphs ($k\leftrightarrow k'$) are not shown, (d) the term $S(k',k,E)$.

FIG. 7. Examples of two-photon amplitudes contributing in the $J = \frac{3}{2}$ channel. Those cannot be obtained by iterating the basic potentials or by their interferences.

FIG. 8. Renormalization graphs of the $\gamma N \Delta$ vertex.

as well as a term corresponding to graph (d) in Fig. 6,

$$S(k',k,E) = \frac{2}{\pi} \int \lambda^2 d\lambda \frac{M}{E_\lambda} \frac{v_{pp}^{\gamma\pi}(k',\lambda)v_{pp}^{\pi\gamma}(\lambda,k)}{E - E_\lambda - \omega_\lambda + i\epsilon} . \quad (44)$$

We can now show that the optical theorem, Eq. (17), is indeed satisfied by explicitly proving that

$$\mathrm{Im}\, t_{\gamma\gamma}(k',k) = -\frac{1}{2\pi} q' \omega_{q'} \cdot \frac{M}{E} \,|\, t_{\pi\gamma}(q',k) \,|^2 \quad (45)$$

with $t_{\gamma\gamma}$ defined by Eq. (40) and $t_{\pi\gamma}$ by Eq. (38). From (45) we immediately get (17) by using (13) and (14). Equations (38) and (40) are the basic formulas needed to calculate the numerical results presented in the last section.

As is obvious from Fig. 6 many different processes are automatically taken into account by Eq. (40). But as a matter of fact, the set of graphs in Fig. 6 is not complete, just as there are graphs contributing to pion scattering, which are not taken into account by Eq. (35). These are graphs which cannot be obtained by iteration of the driving potentials considered here and their interferences. In the case of pion scattering and pion photoproduction some of these graphs can be taken into account in terms of vertex renormalizations as has been done for pion scattering in Ref. 2. Similar renormalizations have to be done for the photon vertices. But unfortunately, vertex renormalizations are not sufficient in the case of Compton scattering. Here, in addition, so-called two-photon amplitudes have to be taken into account. Examples for such two-photon amplitudes, which are neither obtained by iteration of the basic potentials nor by vertex renormalizations, are depicted in Fig. 7. But as has been discussed in a different context,[14] the consideration of those graphs is necessary in order to, e.g., show that the electric multipoles are gauge invariant. Numerically we expect two-photon corrections in the $J = \frac{3}{2}$ channel to be small as are, e.g., also vertex corrections to $f_{\gamma N\Delta}^{(0)}$ (cf. the following section). Therefore we have neglected them here. This is not possible for some other partial waves as will be briefly discussed later.
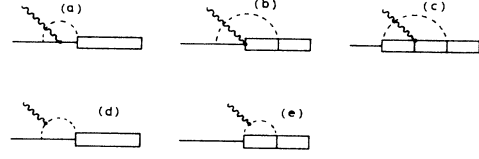
C. Mass and vertex renormalization

The general procedure for renormalizing the CBM has been discussed comprehensively in Ref. 2. We will here follow very closely the procedures outlined there. The renormalized πNN and $\pi N\Delta$ coupling constants $f_{\pi NN}^{(R)}$ and $f_{\pi N\Delta}^{(R)}$ are given by

$$f_{\pi NN}^{(R)} = \frac{V_{\pi NN}(\epsilon)}{Z_N} f_{\pi NN}^{(0)} ,$$

$$f_{\pi N\Delta}^{(R)} = \frac{V_{\pi N\Delta}(\epsilon)}{\sqrt{Z_N}\sqrt{Z_\Delta}} f_{\pi N\Delta}^{(0)} , \quad (46)$$

and explicit expressions for $V_{\pi NN}(\epsilon)$ and $V_{\pi N\Delta}(\epsilon)$ are derived in second-order perturbation theory in Ref. 2.

The quantities Z_N and Z_Δ can be expressed in terms of the nucleon and Δ self-energies, Σ_N and Σ_Δ:

$$Z_N = 1 - \frac{\partial\Sigma_N(E)}{\partial E}\bigg|_{E=M} , \quad (47)$$

$$Z_\Delta = 1 - \frac{\partial\Sigma_\Delta(E)}{\partial E}\bigg|_{E=m_\Delta^{(R)}} . \quad (48)$$

For Σ_N and Σ_Δ we again use the results given in Ref. 2. Explicitly one then gets, for the renormalized Δ mass,

$$m_\Delta^{(R)} = m_\Delta^{(0)} + \Sigma_\Delta(m_\Delta^{(R)}) . \quad (49)$$

As in Ref. 2 $m_\Delta^{(R)}$ has been used as one of the parameters of the model to be fitted.

We now apply the same renormalization procedure to the photon coupling constants $\kappa^{(0)}$ and $f_{\gamma N\Delta}^{(0)}$:

$$\kappa = \frac{V_{\gamma NN}(\epsilon)}{Z_N}\kappa^{(0)}, \quad f_{\gamma N\Delta}^{(R)} = \frac{V_{\gamma N\Delta}(\epsilon)}{\sqrt{Z_N}\sqrt{Z_\Delta}} f_{\gamma N\Delta}^{(0)} . \quad (50)$$

To calculate $V_{\gamma NN}/Z_N$ amounts to evaluating the magnetic moment of the nucleon in the CBM as has been done in Ref. 2. Only the renormalization of $f_{\gamma N\Delta}^{(0)}$ needs some closer consideration. To this end we first calculate the graphs b, c, and e in Fig. 8 in second-order perturbation theory, yielding

$$V_{\gamma N\Delta}(0) = 1 + \frac{5}{3\pi}\frac{f_{\pi NN}^{(0)2}}{m^2}\int_0^\infty dq \frac{q^4 u^2(q)}{\omega_q^2(\omega_q + \omega_\Delta)} + \frac{10}{9\pi}\frac{f_{\pi N\Delta}^{(0)}f_{\pi NN}^{(0)}}{m^2}\int_0^\infty dq \frac{q^4 u^2(q)}{\omega_q(\omega_q + \omega_\Delta)^2}$$

$$+ \frac{5}{6\sqrt{2}\,\pi}\frac{f_{\pi N\Delta}^{(0)}f_{\pi NN}^{(0)}}{m^2\mu_Q}\int_0^\infty dq \frac{q^4 u^2(q)(\omega_\Delta^2 + 7\omega_q\omega_\Delta + 8\omega_q^2)}{\omega_q^2(\omega_q + \omega_\Delta)^2(2\omega_q + \omega_\Delta)} . \quad (51)$$

We neglect the energy dependence of $V_{\gamma N\Delta}$ here and define $\omega_\Delta = m_\Delta^{(0)} - M$. Furthermore, we want to emphasize that the graphs a and d in Fig. 8, which in principle also contribute to the vertex renormalization of $f_{\gamma N\Delta}$ are already accounted for, since they are obtained by iteration of the driving potentials. This is similar, as is discussed in Ref. 2, for the $\pi N\Delta$ vertex. Furthermore, as is shown in detail in that reference for pion scattering, the model is renormalized consistently by the above method; i.e., all unrenormalized quantities appearing in the scattering amplitude (35) are consistently replaced by the corresponding renormalized ones. The same applies for the photoproduction and Compton-scattering amplitudes (38) and (40), respectively.

IV. NUMERICAL RESULTS AND DISCUSSION

The basic results we obtain are predictions for the $M_{1+}(T = \frac{3}{2})$ multipole for photoproduction and the f_{MM}^{1+} multipole of the Compton-scattering amplitude. For both quantities experimental information is available.

Before presenting our results we will briefly outline how the parameters that enter our calculation have been determined. All results, which will be presented, depend on just two parameters: the bag radius R and the mass of the "dressed" Δ (see previous section). The renormalized πNN coupling constant at pion threshold has been set to the experimental value ($f_{\pi NN}^{(R)2} = 0.082$). [Note, that $f_{\pi NN}$ is slightly energy dependent because of Eq. (46).] The parameters are fixed in such a way that the experimental δ_{33} phase shift is reasonably well reproduced. In Fig. 9 our result for the δ_{33} phase shift is shown in comparison to the experimental data of Ref. 15, calculated with

$$R = 0.97 \text{ fm}, \quad m_\Delta^{(R)} = 1242 \text{ MeV} . \quad (52)$$

These values are well in accordance with numbers obtained in other applications of bag models. Our parameters are different from those reported in Ref. 2, since we are using a different πN propagator. The propagator used here has the advantage to correctly take into account nucleon recoil kinematics. We would like to remind the
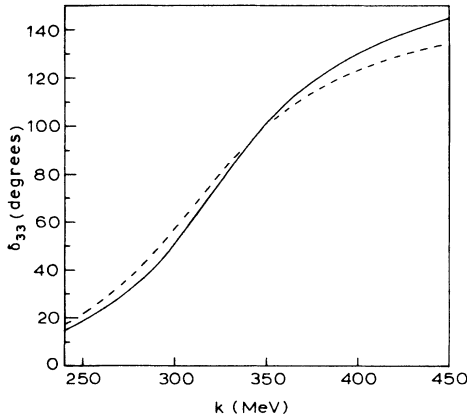

FIG. 9. The δ_{33} phase shift as obtained in this calculation (full line) compared to the data of Ref. 15 (dashed line).

reader that the renormalized Δ mass does not agree with the energy where δ_{33} goes through 90°, since besides the "elementary" Δ we have a Chew-Low background contributing to the scattering in the 33 channel.

We have also performed a calculation with the same πN propagator as in Ref. 2, yielding an even better fit to the δ_{33} phase shift with the parameters

$$R = 0.82 \text{ fm}, \quad m_\Delta^{(R)} = 1278 \text{ MeV}, \quad f_{\pi NN}^{(R)2} = 0.064 . \quad (53)$$

These parameters agree with those reported in Ref. 2 except for $m_\Delta^{(R)}$. Besides the fact that the renormalized $f_{\pi NN}^{(R)}$ appears to be relatively small in this case, comparison of the two calculations shows that the numerical values of the different parameters depend relatively strongly on the πN propagator used. As already remarked in the Introduction this propagator cannot be calculated from the quark model.

The "bare" $\pi N\Delta$ coupling constant is as usual taken from SU(6) symmetry ($f_{\pi N\Delta}^{(0)}/f_{\pi NN}^{(0)} = \sqrt{72/25}$) and renormalization is performed according to Eq. (46). This makes the renormalized $f_{\pi N\Delta}^{(R)}$ slightly energy dependent. As Fig. 9 shows we get a quite reasonable fit to the δ_{33} phase shift with the coupling constants and other parameters determined in this way. The width of the Δ (i.e., the pion scattering cross section in the 33 channel) is a little bit too small as is typical for CBM calculations.

The photon coupling constants $\kappa^{(0)}$ and $f_{\gamma N\Delta}^{(0)}$ are given by Eqs. (29) and (30), and with the parameters (52) they take the value $\kappa^{(0)} = 1.57$ and $f_{\gamma N\Delta}^{(0)} = 0.060$. As has been shown in detail in Refs. 2 and 5, the CBM (with the renormalization procedure discussed in the previous section) reproduces the experimental magnetic moments quite well, if one also includes recoil corrections. Therefore we have taken for renormalized isovector magnetic moment κ simply the experimental value ($\kappa = 2.33$). The renormalized $f_{\gamma N\Delta}^{(R)}$ has been calculated with the parameters (52) and the renormalization procedure (51) to be $f_{\gamma N\Delta}^{(R)} = 0.052$. Here recoil corrections have not been included.

It is possibly interesting to compare this result with other determinations of $f_{\gamma N\Delta}^{(R)}$. In such comparisons some caution has to be exercised, though, since the values have been obtained within different models and the coupling constants are usually not defined in precisely the same way. Koch and Moniz[16] have determined $f_{\gamma N\Delta}^{(R)} = 0.081$ from a phenomenological analysis of pion photoproduction. In that calculation, however, the nonresonant background has been parametrized by a very simple ansatz, so that the quoted value for $f_{\gamma N\Delta}$ should be taken only as a rough guideline. A similar value for $f_{\gamma N\Delta}^{(R)}$ as been used in Ref. 7 ($f_{\gamma N\Delta}^{(R)} = 0.087$ and 0.12). In a very recent analysis of the photoproduction data a value of $f_{\gamma N\Delta}^{(R)} = 0.073$ has been extracted,[17] which seems to be quite in line with the number for $f_{\gamma N\Delta}^{(R)}$, which has been determined recently in another phenomenological analysis[18] of the $\gamma\pi$ process ($f_{\gamma N\Delta}^{(R)} = 0.091$). But as already remarked previously we have to keep in mind that the numerical values for the coupling constants depend relatively strongly on the details of the calculation and the approximations used.

We are now ready to discuss our results for $M_{1+}(T = \frac{3}{2})$ and f_{MM}^{1+}. The $M_{1+}(T = \frac{3}{2})$ multipole is

presented in Fig. 10 and compared to the experimental data from Ref. 15. Obviously the experiment is reproduced quite well by our calculation and, the data seem to be much better accounted for by this calculation than by a previous treatment of the $\gamma\pi$ process within the CBM (Ref. 7). In that calculation Chew-Low processes have been neglected entirely in the 33 channel, and a form factor has been applied at the γ vertices, which is not appropriate for real photons. Another difference to the present calculation is that the Blankenbecler-Sugar reduction of the Bethe-Salpeter equation has been used to iterate the driving potentials.

Our results for the f_{MM}^{1+} multipole are presented in Fig. 11. Here the quality of the available data is much poorer than in the photoproduction case. Nevertheless, some general remarks can be made at this stage. The data given in Fig. 11 are taken from a fit of the multipoles to the available scattering data.[16] As is explained in detail in that reference, the exact values for the f_{MM}^{1+} multipole strongly depend on the conditions under which the fit is performed, so that one may expect that the experimental situation will change when more and better scattering data become available. We also show in Fig. 11 the results of a very elaborate dispersion theoretical calculation of the real part of the f_{MM}^{1+} multipole.[13] As is obvious, the result of the CBM is very similar to the one obtained in the dispersion calculation. That means that, if we take the experimental data at face value, there is a 30—40 % discrepancy between both calculations and the data. This is a serious problem which needs further attention. Note that there is no room to change the parameters in the CBM calculation in any significant way, since all parameters have been fixed to describe pion scattering and photoproduction. This situation certainly seems to be a challenge for both theory and experiment. Concerning theory, one eventually has to ask if the off-shell structure of the pion-scattering amplitude (which determines the photon scattering amplitude) is correctly given by the model employed here. One might, e.g., try to use another
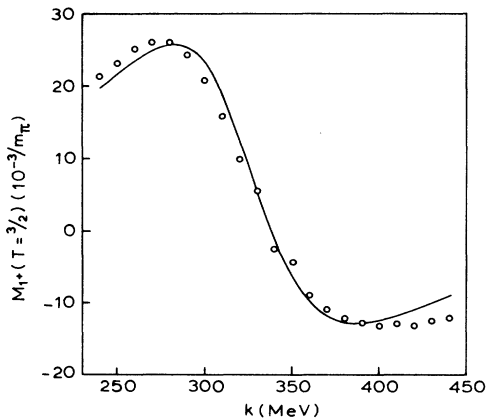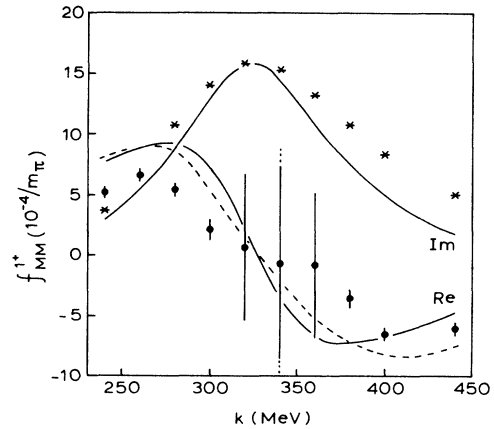

FIG. 11. The f_{MM}^{1+} multipole of the Compton-scattering amplitude: the results of this calculation (full line) compared to the data as obtained by a multipole fit to the scattering cross sections (Ref. 13). Stars represent the imaginary part of the data, full circles represent the real part. The dashed line is the result of the dispersion-theoretical calculation reported in Ref. 13.

(quasi)relativistic equation to iterate the potentials instead of the Lippmann-Schwinger equation employed here. Furthermore, one needs to analyze the predictions of other versions of the CBM, in particular, the version with pseudovector volume coupling of the pion to the bag.[3]

V. CONCLUSIONS AND OUTLOOK

We have attempted in this work a simultaneous description of pion scattering, photoproduction, and Compton scattering within the framework of the CBM. With reasonable values for the parameters of the model we obtain a good description of the δ_{33} phase and the $M_{1+}(T = \frac{3}{2})$ multipole. Watson's theorem is exactly satisfied in this calculation. Since the imaginary part of the Compton-scattering amplitude is directly linked to photoproduction via the optical theorem, we also get an acceptable description of the imaginary part of the f_{MM}^{1+} multipole. The result for the real part of this multipole is off by about 40% as compared to the presently available experimental data. While this situation might change, when better scattering data become available, the discrepancy between model and experiment might also point to some difficulties within the model. In this respect it is important to note that Compton scattering is calculated free of parameters, since all model parameters have been fixed to describe pion scattering and photoproduction.

The CBM provides us with an explicit formulation of the off-shell behavior of the pion-scattering amplitude, which in turn determines the off-shell structure of both photoproduction and Compton scattering. In particular we obtain in this way an explicit model for photon scattering off the nucleon, which resembles quite well the results of dispersion theoretical calculations. One of the

FIG. 10. The real part of the $M_{1+}(T = \frac{3}{2})$ multipole (full line) compared to the data of Ref. 15 (open circles).

advantages of such an explicit model is that it can be applied to calculate Compton scattering of complex nuclei.

We have concentrated our attention here on the Δ resonance region. It would be certainly very interesting to also analyze, how the model behaves at low energies. There the Compton-scattering amplitude is fixed by low-energy theorems up to first order in the photon energy.[19] While for the f_{MM}^{1+} multipole the low-energy theorem is obviously satisfied to zeroth order (i.e., $f_{MM}^{1+} \to 0$ for $k \to 0$), the behavior in first and second order needs to be analyzed carefully. The low-energy behavior will need even more attention, when one considers other partial waves (particularly the electric ones), because the correct low-energy behavior is closely linked to gauge invariance of the Compton amplitude.[19] Especially when considering the f_{EE}^{1+} partial wave we will have to take into account also two-photon amplitudes ("seagull" terms), which do not contribute to f_{MM}^{1+} and are therefore not considered here, in order to have gauge invariance and consequently the low-energy theorem satisfied.

Finally we would like to emphasize that a simultaneous treatment of photon scattering together with pion scattering and photoproduction should also be performed in other versions of the CBM. This may help to get further insight into some features of chiral bag models.

ACKNOWLEDGMENTS

APPENDIX

In this appendix we collect some formulas derived from the CBM, which are useful for evaluating the driving potentials needed in this calculation. Furthermore the propagators entering the different scattering amplitudes are listed. For an explanation of the used symbols see the main text.

The couplings of a pion with isospin α to the "bare" nucleon and Δ are given by

$$H_{\pi NN}^{\alpha}(\mathbf{q}) = i \left[\frac{2\pi}{\omega_q} \right]^{1/2} \frac{f_{\pi NN}^{(0)}}{m} u(q)\sigma \cdot \mathbf{q}\tau_{\alpha} , \tag{A1}$$

$$H_{\pi N\Delta}^{\alpha}(\mathbf{q}) = i \left[\frac{2\pi}{\omega_q} \right]^{1/2} \frac{f_{\pi N\Delta}^{(0)}}{m} u(q)\sigma_{N\Delta} \cdot \mathbf{q}\tau_{N\Delta}^{\alpha} , \tag{A2}$$

$$u(q) = \frac{3j_1(qR)}{qR} . \tag{A3}$$

The couplings of a real photon to the "bare" nucleon and Δ, and the pion are given by

$$H_{\gamma NN}(\mathbf{k}) = \frac{i}{\sqrt{2k}} \frac{e\mu_Q}{2M} \sigma \cdot (\mathbf{k} \times \epsilon_\lambda)\tfrac{1}{6}(1 + 5\tau_3) , \tag{A4}$$

$$H_{\gamma N\Delta}(\mathbf{k}) = \frac{i}{\sqrt{2k}} \frac{e\mu_Q}{2M} \sigma_{N\Delta} \cdot (\mathbf{k} \times \epsilon_\lambda)\sqrt{2}\,\tau_{N\Delta}^3$$

$$= \frac{i}{\sqrt{2k}} \frac{f_{\gamma N\Delta}^{(0)}}{m} \sigma_{N\Delta} \cdot (\mathbf{k} \times \epsilon_\lambda)\tau_{N\Delta}^3 , \tag{A5}$$

$$H_{\gamma\pi\pi}(\mathbf{q},\mathbf{k}) = \frac{i}{\sqrt{2k}} e\epsilon_{\alpha\beta3}\epsilon_\lambda \cdot (2\mathbf{q} + \mathbf{k}), \quad \epsilon_\lambda \cdot \mathbf{k} = 0 . \tag{A6}$$

For the spin and isospin operators σ, $\sigma_{N\Delta}$, τ, and $\tau_{N\Delta}$ we use the following normalization of the reduced matrix elements:

$$\langle \tfrac{1}{2} ||\sigma^{[1]}|| \tfrac{1}{2} \rangle = \sqrt{6}, \quad \langle \tfrac{3}{2} ||\sigma_{\Delta N}^{[1]}|| \tfrac{1}{2} \rangle = 2 . \tag{A7}$$

The propagators D_1, D_2, and D_3 entering the formulas for $t_{\pi\pi}$, $t_{\pi\gamma}$, and $t_{\gamma\gamma}$ take the following form in terms of the πN propagator defined by Eq. (12):

$$D_1(E) = 1 - \frac{2\omega}{\pi} \int_0^\infty d\lambda \, \lambda^2 \frac{M}{E_\lambda} \frac{g^2(\lambda)}{E - E_\lambda - \omega_\lambda + i\epsilon} , \tag{A8}$$

$$D_2(E) = E - m_\Delta^{(0)}$$

$$- \frac{2}{\pi} \int_0^\infty d\lambda \, \lambda^2 \frac{M}{E_\lambda} \frac{h^2(\lambda)}{E - E_\lambda - \omega_\lambda + i\epsilon} , \tag{A9}$$

$$D_3(E) = \frac{2}{\pi} \int_0^\infty d\lambda \, \lambda^2 \frac{M}{E_\lambda} \frac{g(\lambda)h(\lambda)}{E - E_\lambda - \omega_\lambda + i\epsilon} . \tag{A10}$$

[1]G. A. Miller, A. W. Thomas, and S. Théberge, Phys. Lett. 91B, 192 (1980).

[2]S. Théberge, A. W. Thomas, and G. A. Miller, Phys. Rev. D 22, 2838 (1980); 23, 2106(E) (1981); A. W. Thomas, S. Théberge, and G. A. Miller, ibid. 24, 216 (1981).

[3]E. A. Veit, B. K. Jennings, and A. W. Thomas, Phys. Rev. D 33, 1859 (1986).

[4]E. A. Veit, B. K. Jennings, A. W. Thomas, and R. C. Barret, Phys. Rev. D 33, 1033 (1985).

[5]S. Théberge, G. A. Miller, and A. W. Thomas, Can. J. Phys. 60, 59 (1982); S. Théberge and A. W. Thomas, Nucl. Phys. A393, 252 (1983).

[6]K. M. Watson, Phys. Rev. 95, 228 (1954).

[7]M. Araki and A. M. Kamal, Phys. Rev. D 29, 1345 (1983).

[8]G. Kälbermann and J. M. Eisenberg, Phys. Rev. D 28, 71 (1983).

[9]For example, the Brookhaven laser back-scattering facilty.

[10]A. W. Thomas, J. Phys. G 7, L283 (1981).

[11]G. F. Chew and F. E. Low, Phys. Rev. **101**, 157 (1955).

[12]A general definition of the Compton-scattering multipoles is, e.g., given in Y. Nagashima, Prog. Theor. Phys. **33**, 828 (1965).

[13]W. Pfeil, H. Rollnik, and S. Stankowski, Nucl. Phys. **B73**, 166 (1974); S. Stankowski, diploma thesis PIB 2-137, University of Bonn.

[14]J. L. Friar, Phys. Rev. Lett. **36**, 510 (1976); H. Arenhövel, Z. Phys. A **297**, 129 (1980). As discussed in these references, two-photon amplitudes arise if one somehow restricts the space of possible processes. For example, if one does not treat antiparticle degrees of freedom explicitly, they will appear implicitly as a two-photon contribution to the Compton-scattering amplitude. In the calculation presented here we do not treat explicitly $\pi\Delta$ final states, which in turn leads to the two-photon amplitudes mentioned in the main text. The two-photon amplitudes contribute only to the real part of the Compton amplitude.

[15]F. A. Berends and A. Donnachie, Nucl. Phys. **B84**, 342 (1975).

[16]J. H. Koch and E. J. Moniz, Phys. Rev. C **27**, 751 (1983); J. H. Koch, E. J. Moniz, and N. Ohtsuka, Ann. Phys. (N.Y.) **154**, 99 (1984). Note that their $\tilde{g}_{\gamma N\Delta} = 1.04$ is normalized differently than our $f^{(R)}_{\gamma N\Delta}$ and has to be reduced by 30%, since $\tilde{g}_{\gamma N\Delta}$ contains interferences with the Born amplitude.

[17]R. Davidson, N. C. Mukhopadhyay, and R. Wittman, Phys. Rev. Lett. **56**, 804 (1986).

[18]H. Tanabe and K. Ohta, Phys. Rev. C **31**, 1876 (1984).

[19]F. E. Low, Phys. Rev. **96**, 1428 (1954); M. Gell-Mann and M. L. Goldberger, *ibid.* **96**, 1433 (1954).